

Resveratrol reduces light and electron microscopic changes in acetaminophen-induced hepatotoxicity in rats: Role of iNOS expression

Hulya Elbe, Mehmet Gul, Asli Cetin, Elif Taslidere, Fatma Ozyalin, Yusuf Turkoz & Ali Otlu

To cite this article: Hulya Elbe, Mehmet Gul, Asli Cetin, Elif Taslidere, Fatma Ozyalin, Yusuf Turkoz & Ali Otlu (2018) Resveratrol reduces light and electron microscopic changes in acetaminophen-induced hepatotoxicity in rats: Role of iNOS expression, *Ultrastructural Pathology*, 42:1, 39-48, DOI: [10.1080/01913123.2017.1374313](https://doi.org/10.1080/01913123.2017.1374313)

To link to this article: <https://doi.org/10.1080/01913123.2017.1374313>



Published online: 01 Dec 2017.



Submit your article to this journal [↗](#)



Article views: 251



View related articles [↗](#)



View Crossmark data [↗](#)



Citing articles: 2 View citing articles [↗](#)

BASIC RESEARCH



Resveratrol reduces light and electron microscopic changes in acetaminophen-induced hepatotoxicity in rats: Role of iNOS expression

Hulya Elbe^a, Mehmet Gul^b, Asli Cetin^b, Elif Taslidere^c, Fatma Ozyalin^d, Yusuf Turkoz^d, and Ali Otlu^b

^aFaculty of Medicine, Department of Histology and Embryology, Mugla Sıtkı Kocman University, Mugla, Turkey; ^bFaculty of Medicine, Department of Histology and Embryology, Inonu University, Malatya, Turkey; ^cFaculty of Medicine, Department of Histology and Embryology, Bezmialem Vakıf University, Istanbul, Turkey; ^dFaculty of Medicine, Department of Medical Biochemistry, Inonu University, Malatya, Turkey

ABSTRACT

Introduction: Hepatotoxicity is a major complication of acetaminophen (APAP), a widely used analgesic and antipyretic drug. Resveratrol (RSV) is a naturally occurring diphenol and it has anticancer, antioxidant, and anti-inflammatory properties. **Objectives:** In this study, the beneficial effects of RSV on APAP-induced hepatotoxicity was investigated in rats. **Materials and methods:** Group 1: Ethanol, Group 2: Saline, Group 3: RSV (10 mg/kg/ip), Group 4: APAP (1000 mg/kg/ip/single dose), Group 5: APAP+RSV (20 min after administration of APAP). The rats were sacrificed 24 h after administration of APAP. Light and electron microscopic changes were evaluated. Levels of malondialdehyde (MDA) and glutathione (GSH), catalase (CAT), and superoxide dismutase (SOD) activities were determined in liver tissue. **Results:** Rats of the ethanol, saline, and RSV groups did not present any histopathological alterations. In the APAP group, we observed vascular congestion, necrosis, inflammation, sinusoidal dilatation, and loss of glycogen content. In the APAP+RSV group, these changes were markedly reduced. iNOS immunostaining showed very weak positive stained hepatocytes the sections of control, saline, and RSV groups. However, in the APAP group, iNOS immunostaining was most evident in pericentral hepatocytes. In the same areas in APAP+RSV group, intensity of iNOS immunostaining decreased. A significant increase in MDA and decreases in GSH level, CAT, and SOD activity indicated that APAP-induced hepatotoxicity was mediated through oxidative stress. Significant beneficial changes were noted in tissue oxidative stress indicators in rats treated with RSV. **Conclusion:** These biochemical, histopathological, and ultrastructural findings revealed that RSV reduced the severity of APAP-induced alterations in liver.

ARTICLE HISTORY

Received 4 May 2017
Accepted 29 August
Published online 4
December 2017

KEYWORDS

Acetaminophen;
hepatotoxicity; iNOS;
resveratrol

Introduction

Acetaminophen (APAP), otherwise called paracetamol, is used as a regular antipyretic and pain-relieving medication. In general, APAP is safe in therapeutic dosage for people with no history of allergic reaction, liver cirrhosis, and severe renal disease. However, overdose can lead to severe liver and renal necrosis and even death.^{1,2} Under normal conditions, APAP is extensively metabolized by conjugation with glucuronic acid and sulfate in the liver.^{3,4} A little extent of the medication is metabolized by a few of the cytochrome P450 (CYP450) enzymes into the reactive N-acetyl-p-benzoquinone-imine (NAPQI), which is regularly detoxified by glutathione (GSH) both non-enzymatically and enzymatically.⁴ In the abundant of APAP, the amount of sulfate and GSH decreases. This shunts

the excess amount of APAP to the CYP450 mixed-function oxidase system, generating more of the reactive NAPQI.^{4,5} Excess of NAPQI causes oxidative stress and binds covalently to cellular proteins leading to hepatocellular injury.^{4,6}

Resveratrol (3,5,4-trihydroxy-trans-stilbene) is a regularly occurring diphenol available for more than seventy plant species.^{7,8} The richest sources of this compound are grapes, red wine, and peanuts.^{7–9} Results of many studies have provided evidence for its useful effects in animals. The anti-platelet, antioxidant, anti-inflammatory, anticancer, cardioprotective, and proapoptotic properties of resveratrol (RSV) have been well established recently.^{8,9} RSV has been shown to exert an inhibitory effect on reactive oxygen species (ROS) and is a powerful antioxidant.¹⁰

CONTACT Hulya Elbe  h_elbe@hotmail.com  Faculty of Medicine, Department of Histology and Embryology, Mugla Sıtkı Kocman University, 48100, Mugla, Turkey

Color versions of one or more of the figures in the article can be found online at www.tandfonline.com/iusp.

Nitric oxide (NO) is synthesized from L-arginine by three different enzymes: type I: neuronal nitric oxide synthase (NOS), type II: inducible NOS (iNOS), and type III: endothelial NOS (eNOS).^{11–15} NO-mediated cytotoxicity was first defined in macrophages and later on the high concentration of NO was shown to cause apoptosis.¹³ It is explained that NO causes a consecutive loss in mitochondrial membrane potential and thus induces cytochrome c (Cyt c) release to the cytosol.^{14,16,17}

The aim of the present study was to examine the potential beneficial effects of RSV on APAP-induced hepatotoxicity via the role of NO in this process by investigation iNOS expression in rats. Herein, we investigated histopathological, immunohistochemical, and electron microscopic changes, besides measuring oxidative stress indicators in the liver tissue.

Materials and methods

Animals and experimental protocol

Forty Wistar albino male rats (Inonu University Animal Research Center, Malatya, Turkey), weighing between 300 and 350 g, were housed in individual cages in a great ventilated space with a 12:12-hour light/dark cycle at 21°C. Rats were nourished for standard rodent chow and tap water ad libitum. Experiments were performed in accordance with the guidelines for animal research from the National Institute of Health and were approved by the Committee on Animal Research at Inonu University, Malatya, Turkey (Ethical number: 2012-A-03).

Rats were randomly divided into five groups and every group consisted of eight rats as follows: Group 1 (Ethanol): received single intraperitoneally (IP) injection of 4% ethanol, Group 2 (Saline): received single IP injection of saline (0.9%), Group 3 (RSV): received 10 mg/kg/IP single dose of RSV (Sigma-Aldrich, CAS Number: 501–36-0) (RSV was dissolved in isotonic saline 0.9%), Group 4 (APAP): received 1000 mg/kg/IP single dose of APAP (Sigma-Aldrich, CAS Number: 103–90-2) (APAP was dissolved in ethanol), Group 5 (APAP+RSV): RSV was given 20 min after injection of APAP.^{5,8}

Histological evaluation

Rats were sacrificed 24 hours after the treatment with the APAP. Liver tissues were quickly removed and separated into three portions. The first part of the samples was placed in 10% formalin and was embedded in paraffin. Paraffin blocks were sliced at 5 µm and sections were stained with hematoxylin-eosin (H-E) to evaluate the general liver structure and Periodic Acid Schiff (PAS) to demonstrate the glycogen deposition in hepatocytes. The sections were evaluated for severity of liver damage such as infiltration, sinusoidal dilatation, necrosis, congestion, and for the loss of glycogen content of hepatocytes. For the analysis of liver damage, every slide was semiquantitatively graded as follows: absent (0), mild (1), moderate (2), and severe (3). The maximum score was 15.

Immunohistochemical (IHC) evaluation

The sections were mounted on polylysine-covered slides. After rehydrating, specimens were exchanged on citrate buffer (pH 7.6) and warmed in a microwave oven for 20 minutes. Then, after cooling for 20 minutes at room temperature, those areas were washed with phosphate buffered saline (PBS). Then sections were kept in 3% hydrogen peroxide for 7 minutes and subsequently washed with PBS. Sections were incubated with primary rabbit-polyclonal iNOS antibody (dilution 1:100) (Abcam, ab136918) for 60 minutes. They were then rinsed in PBS and incubated with biotinylated goat anti-rabbit polyvalent antibody for 10 minutes and streptavidin peroxidase for 10 minutes at room temperature. Polyvalent HRP Kit (Ready-To-Use) (Patolab, PL-0125-HRP) was used according to the manufacturer's instructions. Staining was completed with chromogen + substrate for 15 minutes, and slides were counterstained with Mayer's hematoxylin for 1 minute, rinsed in tap water, and dehydrated. Brown-yellow granules in cytoplasm or nuclei were recognized as positive staining for iNOS. Cytoplasmic stainings with iNOS were revealed to be positive.¹⁸ The relative intensity of iNOS immunostaining within cells was scored as follows: absent (0), slight (1), moderate (2), and severe (3). All sections were examined using a Leica DFC280 light microscope

and a Leica Q-Win Image Analysis system (Leica Micros Imaging Solutions Ltd., Cambridge, UK).

Transmission electron microscopic evaluation

Tissue specimens were fixed in glutaraldehyde (2.5%) buffered with 0.2 M $\text{NaH}_2\text{PO}_4 + \text{NaHPO}_4$ (pH = 7.2–7.3) and post-fixed in OsO_4 (1%). After dehydration in acetone, they were embedded in Araldite CY212. Ultrathin sections were stained with uranyl acetic acid derivation and lead citrate than were analyzed in a Zeiss Libra 120 (Carl Zeiss NTS, Oberkochen, Germany) electron microscope.¹⁹

Biochemical analysis

The tissue samples were homogenized in ice-cold 0.1 M Tris-hydrochloride buffer (pH 7.5) with a homogenizer at 16,000 rpm for 2 min at +4 to 8°C. Malondialdehyde (MDA), indicated as thiobarbituric acid reactive substances (TBARS), was measured with thiobarbituric acid at 535–520 nm in a spectrophotometer.²⁰ Reduced GSH assay in the homogenates was measured according to the Ellman's method.²¹ Results were stated as nmol/g/wet tissue. Superoxide dismutase (SOD) activity was measured by determining the reduction of nitroblue tetrazolium by the superoxide anion produced by xanthine and xanthine oxidase.²² The activity of the enzyme was expressed in units per gram (U/g) protein. Proteins in the liver tissue were determined by

the method of Lowry et al.²³ Catalase (CAT) activity was measured by determination of the rate constant k (dimension: s^{-1} , k) of hydrogen peroxide (initial concentration 10 mM) at 240 nm in the spectrophotometer.²⁴ The activity of the enzyme was stated as k (concentrate) per gram (k/g) protein.

Statistical analysis

The analysis was carried out using the SPSS 13.0 statistical program. All data are expressed as the arithmetic mean \pm standard error (SE). Normality for continued variables in groups was determined by the Shapiro–Wilk test. Kruskal–Wallis and Mann–Whitney U tests were used for comparison of variables among the studied groups. $p < 0.05$ was regarded as significant.

Results

Histological findings

Sections of the ethanol, saline, and RSV groups did not present any histopathological alterations (Figure 1). There was no significant difference among these groups ($p > 0.05$). The liver tissues of the APAP group showed prominent portal and lobular changes including vascular congestion, necrosis, portal and focal inflammation, sinusoidal dilatation, and loss of glycogen content (Figure 2 (a–d)). The mean histopathological damage score (MHDS) was 6.62 ± 0.37 in APAP group. There

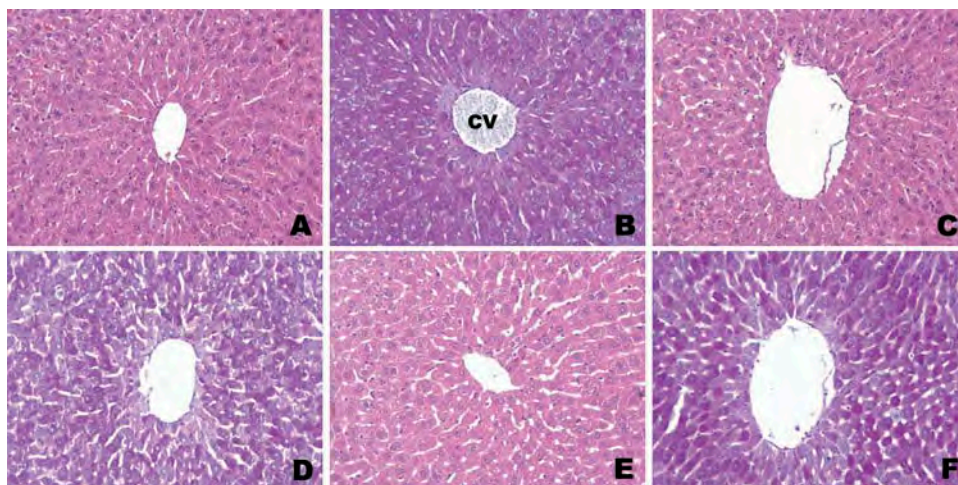


Figure 1. Photomicrographs of liver tissue of control rats showing normal hepatic cells with central vein (CV). A. Group 1: Ethanol group. H-E; X20. B. Group 1: Ethanol group. PAS; X20. C. Group 2: Saline group. H-E; X20. D. Group 2: Saline group. PAS; X20. E. Group 3: RSV group. H-E; X20. F. Group 3: RSV group. PAS; X20.

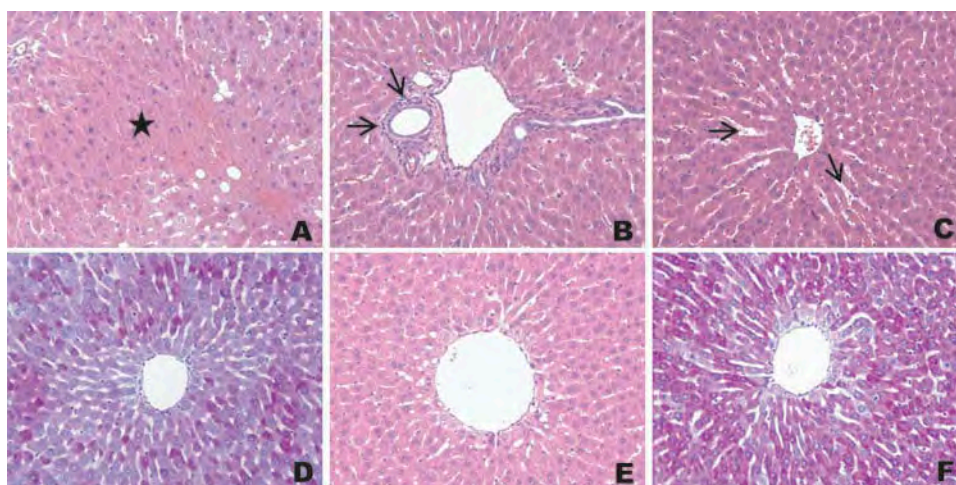


Figure 2. Photomicrographs of liver tissue of rats treated with acetaminophen. A. Group 4: APAP group showing severe necrosis (star) with disappearance of nuclei. H-E; X20. B. Group 4: APAP group showing inflammation areas (arrows). H-E; X20. C. Group 4: APAP group showing sinusoidal dilatation (arrows). H-E; X20. D. Group 4: APAP group showing loss of glycogen content. PAS; X20. E. Group 5: RSV administration ameliorates histopathological changes markedly in APAP-treated rat livers. H-E; X20. F. Group 5: APAP+RSV group showing loss of glycogen content, PAS; X20.

were significant differences between APAP and ethanol, saline, RSV groups ($p = 0.001$, for all). In the APAP+RSV group, these changes were markedly reduced. Rarely, small necrotic hepatocyte groups among normal-appearing hepatocytes were observed. Sinusoidal dilatation was not distinct (Figure 2(e)). Loss of glycogen content was still prominent in PAS-stained sections (Figure 2(f)). MHDS was 3.37 ± 0.32 in APAP+RSV group. There was a significant difference between the APAP and APAP+RSV groups ($p = 0.001$). MHDSs of the groups are shown in Table 1.

Immunohistochemical findings

The livers of ethanol, saline, and RSV groups showed very weak iNOS expression. There were no significant differences between these groups ($p > 0.05$). However, livers of the APAP group showed intense iNOS expression than ethanol, saline and RSV groups ($p < 0.05$). In APAP group, iNOS immunostaining was most evident in pericentral hepatocytes. There were significant

differences between APAP group and ethanol, saline, RSV groups ($p < 0.0001$, $p < 0.0001$, $p = 0.001$, respectively). In the same areas in APAP+RSV group, the intensity of iNOS immunostaining decreased with RSV administration, when compared to APAP group ($p = 0.003$) (Figure 3). The iNOS immunostaining scores are shown in Table 2.

Electron microscopic findings

Liver sections of ethanol, saline, and RSV groups showed normal ultrastructural appearance. Conversely, severe changes were detected in APAP group including minimal intracytoplasmic edema, lipid droplets in hepatocytes, granular material accumulation, and closure in the space of Disse, sinusoidal endothelial degeneration, dense heterogeneous lysosomal accumulation in Kupffer cells, and locally degenerated Kupffer cells. Additionally, in this group, we also observed myelin figures within hydropic vacuoles in perinuclear area and condensation in the

Table 1. The mean histopathological damage score (MHDS) of all groups.

	Ethanol	Saline	RSV	APAP	APAP + RSV
MHDS	0.50 ± 0.26	0.37 ± 0.18	0.37 ± 0.18	6.62 ± 0.37^a	3.37 ± 0.32^b

Data are expressed mean \pm SE ($n = 8$).

^a $p = 0.001$ vs. ethanol, saline, and RSV group

^b $p = 0.001$ vs. APAP group.

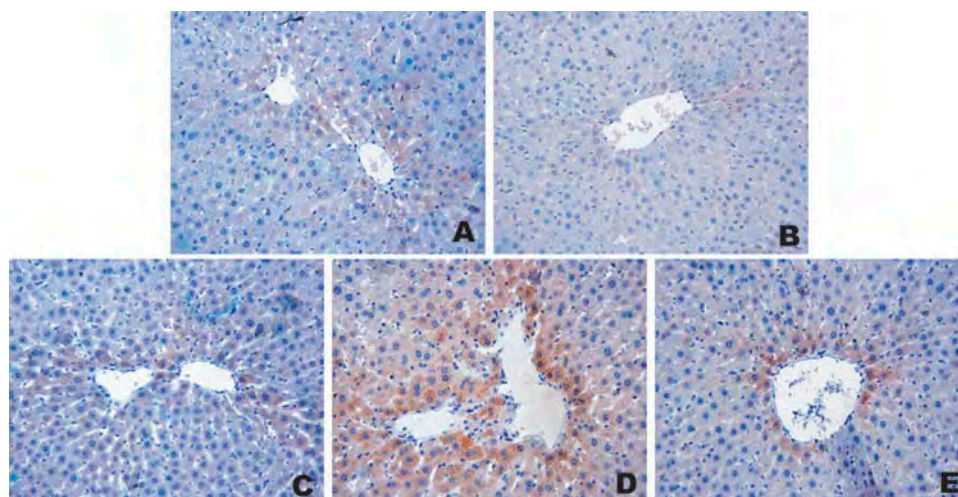


Figure 3. Immunohistochemical photomicrographs of liver tissue of rats for iNOS expression. The areas stained in brown indicated iNOS positive expression. The livers of ethanol, saline, and RSV groups showed very weak iNOS expression. A. Group 1: Ethanol group, X20. B. Group 2: Saline group, X20. C. Group 3: RSV group, X20. D. Group 4: APAP group showing most evident iNOS immunostaining in pericentral hepatocytes, X20. E. Group 5: APAP+RSV group showing that the intensity of iNOS immunostaining decreased with RSV administration, X20.

Table 2. The iNOS immunostaining scores of all groups.

	Ethanol	Saline	RSV	APAP	APAP + RSV
Score	0.25 ± 0.16	0.12 ± 0.12	0.37 ± 0.18	2.50 ± 0.18 ^{a,b}	1.37 ± 0.18 ^{c,d,e,f}

Data are expressed mean ± SE ($n = 8$).

^a $p < 0.0001$ vs. ethanol and saline group.

^b $p = 0.001$ vs. RSV group.

^c $p = 0.002$ vs. ethanol group.

^d $p = 0.001$ vs. saline group.

^e $p = 0.005$ vs. RSV group.

^f $p = 0.003$ vs. APAP group.

mitochondrial matrix. Liver sections of APAP+RSV group were nearly normal in ultrastructural appearances. In this group, small lysosomes, rarely small myelin figures in hepatocyte cytoplasm, and locally minimal intracytoplasmic edema were observed (Figure 4).

Biochemical findings

The tissue MDA levels of APAP group were significantly increased in comparison with ethanol, saline, and RSV groups ($p < 0.05$, $p < 0.05$, $p < 0.005$, respectively). However, tissue MDA levels of APAP+RSV group was significantly lower than that of APAP group ($p < 0.05$). When compared with the ethanol, saline, and RSV groups, tissue GSH levels, SOD, and CAT activity in APAP group were significantly decreased. RSV administration resulted in a significant increase in mean GSH level, CAT, and SOD activities

($p < 0.05$, $p < 0.01$, $p < 0.005$, respectively). The mean biochemical results of all groups are shown in Table 3.

Discussion

Despite APAP being an antipyretic and pain-relieving anti-inflammatory drug, which is broadly used to treat cerebral pain, fever, and other pains, and promptly accessible without a prescription, when taken in heavy doses, it becomes an intense hepatotoxin and causes acute liver dysfunction in humans and experimental animals.²⁵ APAP is one of the most common reasons of drug-induced hepatic toxicity around the world that leads to excessive treatment and hospitalization costs every year.²⁶

In the present study, hepatic damage of APAP group was higher than other groups. Placke et al. reported that in mice given 600 mg/kg single dose

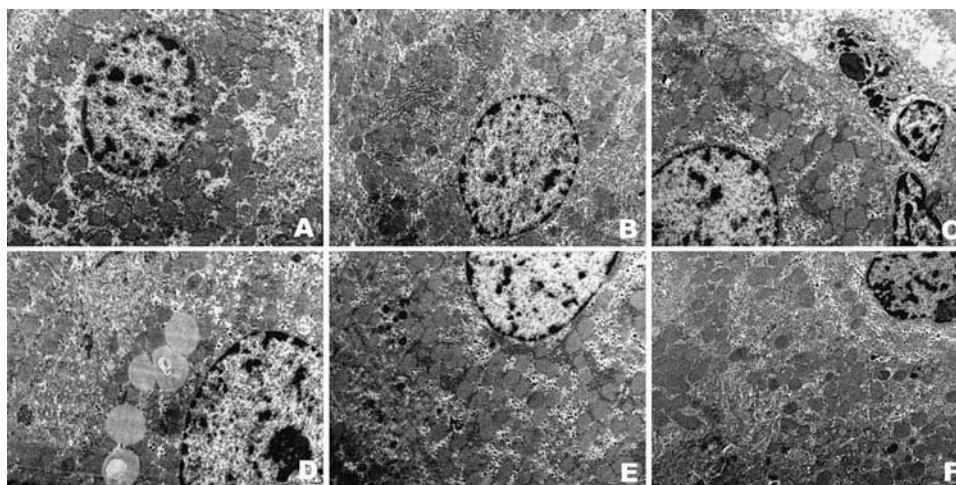


Figure 4. Transmission Electron Microscopic (TEM) photomicrographs of liver tissue of rats. Liver sections of ethanol, saline, and RSV groups showing normal ultrastructural appearance. A. Group 1: Ethanol group, X6300. B. Group 3: RSV group, X6300. C. Group 4: APAP group showing minimal intracytoplasmic edema, lipid droplets in hepatocytes, granular material accumulation, and myelin figures within hydropic vacuoles in perinuclear area, X6300. D. Group 4: APAP group showing intracytoplasmic edema and lipid droplets, X8000. E. F. Group 5: APAP + RSV group showing small lysosomes, rarely small myelin figures in hepatocyte cytoplasm and locally minimal intracytoplasmic edema X6300.

Table 3. The tissue oxidant–antioxidant parameters of all groups.

	MDA (nmol/g wet tissue)	GSH (nmol/g wet tissue)	SOD (U/g protein)	CAT (k/g protein)
Ethanol	362.00 ± 5.87	1.28 ± 0.14	115.87 ± 3.54	22.00 ± 0.32
Saline	374.12 ± 12.10	1.24 ± 0.09	119.50 ± 3.90	24.68 ± 0.52 ^g
RSV	336.75 ± 4.29 ^{a,b}	1.29 ± 0.04	152.75 ± 7.02 ^{g,h}	30.42 ± 0.60 ^{b,g}
APAP	464.25 ± 23.11 ^{c,d}	0.89 ± 0.13 ^{c,d}	104.37 ± 11.48 ⁱ	19.97 ± 1.35 ^{d,j}
APAP + RSV	384.12 ± 24.02 ^e	1.47 ± 0.10 ^f	161.75 ± 7.66 ^e	27.78 ± 1.72 ^k

Data are expressed mean ± SE ($n = 8$).

^a $p < 0.05$ vs. ethanol group.

^b $p < 0.005$ vs. saline group.

^c $p < 0.05$ vs. ethanol and saline group.

^d $p < 0.005$ vs. RSV group.

^e $p < 0.05$ vs. APAP group.

^f $p < 0.005$ vs. APAP group.

^g $p < 0.005$ vs. ethanol group.

^h $p < 0.01$ vs. saline group.

ⁱ $p < 0.01$ vs. RSV group.

^j $p < 0.05$ vs. saline group.

^k $p < 0.01$ vs. APAP group

of APAP at 60 minutes, alterations started for hydropic degeneration, followed by pyknosis, coagulative necrosis, and hepatocellular atrophy.²⁷ Dash et al. reported that in paracetamol-treated group, severe hepatotoxicity was observed by severe necrosis with the disappearance of nuclei.²⁸ Hussain et al. also observed severe congestion of blood vessels alongside vacuolization, hepatic cell necrosis, plasma cells infiltration, macrophages, eosinophils, degeneration of hepatocytes nuclei, and fibrosis.²⁹ Khayyat et al. reported that liver specimens from mice in the APAP-administered group showed diffuse coagulative necrosis around

the vena centralis. Necrotic areas were characterized by eosinophilic, vacuolated, swollen hepatocytes.²⁶ Wu et al. reported that in the APAP group, severe hemorrhage, sinusoidal congestion, and inflammatory cell infiltration dilated central vein and degenerated hepatocytes with perinuclear vacuolization.³⁰ Polat et al. also seen similar histopathological alterations including intense necrotic foci, an increase of eosinophils, irregular Remark cordons, dilated sinusoids, intense erythrocyte aggregation, severe hyperchromasia in the nucleus, and irregularity of the cell membrane in hepatocytes of the liver tissue, which

were given paracetamol.³¹ Our results are concordant with the literature.

The use of natural products in the treatment of *in vivo* and *in vitro* rodent models of liver injury including APAP-induced hepatotoxicity is popular.^{25,28,29,32,33} Among these products, RSV has been shown to be a powerful antioxidant and free radical scavenger.³⁴ RSV provides protection against liver injury induced by ROS and inflammatory cytokines and decreases hepatic lipid peroxidation.³⁵ In previous studies, it was stated that RSV has beneficial effects on different liver injuries.^{35–43} In our study, RSV significantly improved light and electron microscopic alterations against detrimental effects of high-dose administration of APAP. It was suggested that RSV protected against APAP-induced liver toxicity due to its antioxidative and anti-inflammatory effects. McGill et al. reported that inflammation plays a significant role in APAP-induced liver toxicity and that RSV protected by decreasing inflammation.³⁴ Du et al. (2015) reported that RSV prevents histopathological changes in APAP-induced liver injury. Additionally, they emphasize that RSV may be a valid treatment option for APAP overdose.⁴⁴ Wang et al. reported that centrilobular hepatocellular necrosis, intrahepatic hemorrhage, and inflammatory cell infiltration were observed in APAP-induced hepatotoxicity and RSV pretreatment for three days before APAP treatment prevents against liver injury.²⁵

NO is a significant indication of the inflammatory process.⁴⁵ In a variety of cells including neutrophils, macrophages, and hepatocytes, iNOS is induced by inflammatory cytokines.^{46,47} The expression of iNOS leads to overproduction of NO, resulting in damage to neuronal, endothelial, and epithelial cells⁴⁷ and it has been shown to be an important event in various models of liver injury.^{46,47} NO reacts with superoxide radicals, the formation of peroxynitrite by rapid reaction of superoxide anion and NO mediates nitrotyrosination.^{45,47} Peroxynitrite causes protein nitration and tissue injury.⁴⁷ During detoxification of peroxynitrite, GSH has an important role.⁴⁵ In the current study, we observed a correlation between NO synthesis and APAP-induced liver damage as examined by the anti-iNOS intensity

in IHC-stained specimens. Previous studies have also reported that toxic doses of APAP lead to induction of the iNOS and nitrotyrosine expression and increased tissue NO levels and serum nitrite/nitrate levels.^{45,46,48–50} Gardner et al. reported that cells isolated from APAP-treated (1 g/kg) rats produced more NO than cells from control animals. They concluded that NO is a significant indicator of APAP-induced hepatic toxicity.⁴⁸

Ultrastructural studies related to APAP-induced hepatic injury are limited. Placke et al. reported that time- and dose-dependent (300 mg/kg and 600 mg/kg) ultrastructural changes were detected in APAP-induced hepatic damage in mice. The first ultrastructural changes (600 mg/kg of APAP single dose) on hepatocytes were seen at 60 minutes. These cells had mild cytomegaly, decreased density, and dispersion of organelles. Mitochondria were compressed and were occasionally combined with little myelin figures. Those little intracristal calcium granules typically connected with mitochondria were not observed. Most of the endoplasmic reticulum was mildly elongated, round, or dilated. Centrilobular hepatocytes from mice killed 4–6 hours following APAP were necrotic and degeneration had extended into mid zonal and periportal zones.²⁷ In current study, we used 1000 mg/kg single dose of APAP and we detected similar ultrastructural changes at 60 minutes. We could not find any electron microscopic studies related with the role of RSV against APAP-induced hepatotoxicity in literature. Taken all together, we suggest that ultrastructural changes were commonly associated with higher APAP dose and RSV is excessively effective in improvement of ultrastructural damage. Although the precise mechanism by which APAP causes cell injury is still unknown. When we consider all of these light and electron microscopic changes, it is suggested that mitochondria may play a significant role in the APAP-induced hepatic injury.

Oxidative stress has been hypothesized by many researchers to play a significant role in the etiology of APAP toxicity.^{26,31} APAP hepatotoxicity is defined as an imbalance between the production of ROS, antioxidants, and repair capacity.²⁶ MDA level is an important biomarker of lipid peroxidation and its increase in tissues, exposed to oxidative stress.^{26,31,45}

MDA level elevation during APAP toxicity has been reported in the literature.²⁶ Several studies have indicated that APAP might involve free radicals and induce oxidative injury.^{5,26,28,30–33,45,49} As a free radical scavenger, GSH plays a significant role in the detoxification of ROS.^{31,51} Our study showed that RSV decreased levels of MDA and increased levels of hepatic antioxidant enzymes. We suggest that RSV decreases oxidative stress by directly scavenging free radicals and by upregulating antioxidant enzymes, including SOD and CAT. RSV acts as an antioxidant and it is effective in normalization of the antioxidant enzyme system. Wang et al. reported that APAP (400 mg/kg) treatment for 6 hours caused a significant decrease in liver mitochondrial GSH levels, which was reversed by RSV pretreatment.²⁵ Sener et al. reported that a single dose of 900 mg/kg APAP hepatotoxicity was reduced by RSV in BALB-c mice. They determined that APAP caused a significant decrease in GSH levels while MDA levels were increased in liver. Conversely, when RSV administered following APAP, depletion of GSH and accumulation of MDA and neutrophil infiltration were reversed back to control.³³ Our results are concordant with the literature.

Conclusion

We concluded that all of the histological and biochemical changes in APAP hepatotoxicity may be mediated by either lipid peroxidation or by peroxynitrite. We suggest that RSV has a potent effect against APAP-induced hepatic damage by providing the normalization of the antioxidant enzyme system. These findings emphasize the important role of dietary natural substances and offer an innovative approach to coping with APAP-induced hepatotoxicity. Thus it may have potential beneficial effects in protection against the dose-dependent APAP administrations in patients. Further investigations should be conducted to untie the role of dietary compounds which are becoming more remarkable as alternative therapies.

Declaration of interest

The authors declare no conflicts of interest.

Funding

This study was financially supported by Scientific Research Fund of Inonu University, Turkey [Grant number: 2012/85].

References

1. Ghosh A, Sil PC. Antioxidative effect of a protein from *Cajanus indicus* L against acetaminophen-induced hepato-nephro toxicity. *J Biochem Mol Biol.* 2007;40(6):1039–1049.
2. Galal RM, Zaki HF, Seif El-Nasr MM, Agha AM. Potential protective effect of honey against paracetamol-induced hepatotoxicity. *Arch Iran Med.* 2012;15(11):674–680.
3. Chen X, Sun C-K, Han G-Z, et al. Protective effect of tea polyphenols against paracetamol-induced hepatotoxicity in mice is significantly correlated with cytochrome P450 suppression. *World J Gastroenterol.* 2009;15(15):1829–1835.
4. Singh SK, Rajasekar N, Raj NAV, Paramaguru R. Hepatoprotective and antioxidant effects of *Amorphophallus campanulatus* against acetaminophen-induced hepatotoxicity in rats. *Int J Pharm Pharm Sci.* 2011;3(2):202–205.
5. Ilbey YO, Ozbek E, Cekmen M, et al. Melatonin prevents acetaminophen-induced nephrotoxicity in rats. *Int Urol Nephrol.* 2009;41:695–702.
6. Gamal El-Din AM, Mostafa AM, Al-Shabanah OA, Al-Bekairi AM, Nagi MN. Protective effect of arabic gum against acetaminophen-induced hepatotoxicity in mice. *Pharmacological Res.* 2003;48:631–635.
7. Cao Y, Fu Z-D, Wang F, Liu H-Y, Han R. Anti-angiogenic activity of resveratrol, a natural compound from medicinal plants. *J Asian Nat Prod Res.* 2005;7(3):205–213.
8. Yar AS, Menevse S, Alp E, Helvacioğlu F, Take G. The effects of resveratrol on cyclooxygenase-1 and cyclooxygenase-2 mRNA and protein levels in diabetic rat kidneys. *Mol Biol Rep.* 2010;37:2323–2331.
9. Szkudelski T. Resveratrol-induced inhibition of insulin secretion from rat pancreatic islets: Evidence for pivotal role of metabolic disturbances. *Am J Physiol Endocrinol Metab.* 2007;293:901–907.
10. Hung L-M, Chen J-K, Huang -S-S, Lee R-S, Su M-J. Cardioprotective effect of resveratrol, a natural antioxidant derived from grapes. *Cardiovasc Res.* 2000;47:549–555.
11. Ignarro LJ, Buga GM, Wood KS, Byrns RE, Chaudhuri G. Endothelium-derived relaxing factor produced and released from artery and vein is nitric oxide. *Proc Natl Acad Sci USA.* 1987;84:9265–9269.
12. Nathan C. Nitric oxide as a secretory product of mammalian cells. *Faseb J.* 1992;6:3051–3064.

13. Hibbs JBJ, Taintor RR, Vavrin Z. Macrophage cytotoxicity: role for L-arginine deiminase and imino nitrogen oxidation to nitrite. *Sci*. 1987;235:473–476.
14. Bonfoco E, Krainc D, Ankarcrona M, Nicotera P, Lipton SA. Apoptosis and necrosis: Two distinct events induced, respectively, by mild and intense insults with N-methyl D-aspartate or nitric oxide/superoxide in cortical cell cultures. *Proc Natl Acad Sci USA*. 1995;92:7162–7166.
15. Dincel GC, Kul O. eNOS and iNOS trigger apoptosis in the brains of sheep and goats naturally infected with the border disease virus. *Histol Histopathol*. 2015;30(10):1233–1242.
16. Brookes PS, Salinas EP, Darley-Usmar K, et al. Concentration-dependent effects of nitric oxide on mitochondrial permeability transition and cytochrome c release. *J Biol Chem*. 2000;275:20474–20479.
17. Moriya R, Uehara T, Nomura Y. Mechanism of nitric oxide-induced apoptosis in human neuroblastoma SH-SY5Y cells. *FEBS Lett*. 2000;484:253–260.
18. Özer MA, Polat N, Özen S, et al. Effects of molsidomine on retinopathy and oxidative stress induced by radiotherapy in rat eyes. *Curr Eye Res*. 2017;42(5):803–809.
19. Gul M, Kayhan B, Elbe H, Dogan Z, Otlu A. Histological and biochemical effects of dexmedetomidine on liver during an inflammatory bowel disease. *Ultrastruct Pathol*. 2015;39(1):6–12.
20. Uchiyama M, Mihara M. Determination of malonaldehyde precursor in tissues by thiobarbituric acid test. *Anal Biochem*. 1978;86(1):271–278.
21. Ellman GL. Tissue sulphhydryl groups. *Arch Biochem Biophys*. 1959;82:70–77.
22. Sun Y, Oberly LW, Li Y. A simple method for clinical assay of SOD. *Clin Chem*. 1988;34:479–500.
23. Lowry O, Rosenbraugh N, Farr L, Rondell R. Protein measurement with the folin-phenol reagent. *J Biol Chem*. 1951;183:265–275.
24. Casado A, De La Torre R, Lopéz-Fernández E. Antioxidant enzyme levels in red blood cells from cataract patients. *Gerontol*. 2001;47:186–188.
25. Wang Y, Jiang Y, Fan X, et al. Hepato-protective effect of resveratrol against acetaminophen-induced liver injury is associated with inhibition of CYP-mediated bioactivation and regulation of SIRT1–p53 signaling pathways. *Toxicol Lett*. 2015;236:82–89.
26. Khayyat A, Tobwala S, Hart M, Ercal N. N-acetylcysteine amide, a promising antidote for acetaminophen toxicity. *Toxicol Lett*. 2016;241:133–142.
27. Placke ME, Ginsberg GL, Wyand SD, Cohen SD. Ultrastructural changes during acute acetaminophen-induced hepatotoxicity in the mouse: a time and dose study. *Toxicol Pathol*. 1987;15:431–438.
28. Dash DK, Yeligar VC, Nayak SS, et al. Evaluation of hepatoprotective and antioxidant activity of *Ichnocarpus frutescens* (Linn.) R.Br. on paracetamol-induced hepatotoxicity in rats. *Trop J Pharm Res*. 2007 September;6(3):755–765.
29. Hussain L, Ikram J, Rehman K, Tariq M, Ibrahim M, Akash MSH. Hepatoprotective effects of *Malva sylvestris* L. against paracetamol-induced hepatotoxicity. *Turk J Biol*. 2014;38:396–402.
30. Wu Y-L, Piao D-M, Han X-H, Nan J-X. Protective effects of salidroside against acetaminophen-induced toxicity in mice. *Biol Pharm Bull*. 2008;31(8):1523–1529.
31. Polat M, Cerrah S, Albayrak B, et al. Assessing the effect of leptin on liver damage in case of hepatic injury associated with paracetamol poisoning. *Gastroenterol Res Pract*. 2015;357360. DOI:10.1155/2015/357360
32. Pang C, Zheng Z, Shi L, et al. Caffeic acid prevents acetaminophen-induced liver injury by activating the Keap1-Nrf2 antioxidative defense system. *Free Radic Biol Med*. 2016;91:236–246.
33. Sener G, Toklu HZ, Sehirli AO, Velioglu-Ogünç A, Cetinel S, Gedik N. Protective effects of resveratrol against acetaminophen-induced toxicity in mice. *Hepatol Res*. 2006;35(1):62–68.
34. McGill MR, Du K, Weemhoff JL, Jaeschke H. Critical review of resveratrol in xenobiotic-induced hepatotoxicity. *Food Chem Toxicol*. 2015;86:309–318.
35. Dalaklioglu S, Genc GE, Aksoy NH, Akcıt F, Gumuslu S. Resveratrol ameliorates methotrexate-induced hepatotoxicity in rats via inhibition of lipid peroxidation. *Hum Exp Toxicol*. 2013;32(6):662–671.
36. Chan CC, Cheng LY, Lin CL, Huang YH, Lin HC, Lee FY. The protective role of natural phytoalexin resveratrol on inflammation, fibrosis and regeneration in cholestatic liver injury. *Mol Nutr Food Res*. 2011;55(12):1841–1849.
37. Chan CC, Lee KC, Huang YH, Chou CK, Lin HC, Lee FY. Regulation by resveratrol of the cellular factors mediating liver damage and regeneration after acute toxic liver injury. *J Gastroenterol Hepatol*. 2014;29(3):603–613.
38. Lee ES, Shin MO, Yoon S, Moon JO. Resveratrol inhibits dimethylnitrosamine-induced hepatic fibrosis in rats. *Arch Pharm Res*. 2010;33(6):925–932.
39. Oliva J, French BA, Li J, Bardag-Gorce F, Fu P, French SW. Sirt1 is involved in energy metabolism: The role of chronic ethanol feeding and resveratrol. *Exp Mol Pathol*. 2008;85(3):155–159.
40. Tunali-Akbay T, Sehirli O, Ercan F, Sener G. Resveratrol protects against methotrexate-induced hepatic injury in rats. *J Pharm Pharm Sci*. 2010;13(2):303–310.
41. Nivet-Antoine V, Cottart CH, Lemaréchal H, et al. Trans-resveratrol downregulates Txnip overexpression occurring during liver ischemia-reperfusion. *Biochimie*. 2010;92(12):1766–1771.

42. Roy S, Sannigrahi S, Majumdar S, Ghosh B, Sarkar B. Resveratrol regulates antioxidant status, inhibits cytokine expression and restricts apoptosis in carbon tetrachloride induced rat hepatic injury. *Oxid Med Cell Longev*. 2011;2011:703676.
43. Velioglu-Ogunc A, Sehirlı O, Toklu H, et al. Resveratrol protects against irradiation-induced hepatic and ileal damage via its antioxidative activity. *Free Rad Res*. 2009;43:1060–1071.
44. Du K, McGill MR, Xie Y, Bajt ML, Jaeschke H. Resveratrol prevents protein nitration and release of endonucleases from mitochondria during acetaminophen hepatotoxicity. *Food Chem Toxicol*. 2015;81:62–70.
45. Kuvandik G, Duru M, Nacar A, et al. Effects of erdos-teine on acetaminophen-induced hepatotoxicity in rats. *Toxicol Pathol*. 2008;36:714–719.
46. Gardner CR, Laskin JD, Dambach DM, et al. Reduced hepatotoxicity of acetaminophen in mice lacking inducible nitric oxide synthase: potential role of tumor necrosis factor- α and interleukin-10. *Toxicol Appl Pharmacol*. 2002;184:27–36.
47. Kamanakaa Y, Kawabatab A, Matsuyaa H, Tagaa C, Sekiguchib F, Kawao N. Effect of a potent iNOS inhibitor (ONO-1714) on acetaminophen-induced hepatotoxicity in the rat. *Life Sci*. 2003;74:793–802.
48. Gardner CR, Heck DE, Yang CS, et al. Role of nitric oxide in acetaminophen-induced hepatotoxicity in the rat. *Hepatol*. 1998;26:748–754.
49. Hinson JA, Bucci TJ, Irwin LK, Michael SL, Mayeux PR. Effect of inhibitors of nitric oxide synthase on acetaminophen-induced hepatotoxicity in mice. *Nitric Oxide: Biol Chem*. 2002;6(2):160–167.
50. Zhao YL, Zhou GD, Yang HB, et al. Rhein protects against acetaminophen-induced hepatic and renal toxicity. *Food Chem Toxicol*. 2011;49(8):1705–1710.
51. Mutlib AE, Shockcor J, Espina R, et al. Disposition of glutathione conjugates in rats by a novel glutamic acid pathway: Characterization of unique peptide conjugates by liquid chromatography/mass spectrometry and liquid chromatography/NMR. *J Pharm Exp Ther*. 2000;235:25–32.